energy&fuels

pubs.acs.org/EF

Article

Improved CO_2 Separation Using Aqueous Solutions of 2-Amino-2-hydroxymethyl-1,3-propanediol Promoted with Piperazine

Shaurya Mohan, Namrata Upreti, and Prakash D. Vaidya*

Cite This: *Energy Fuels* 2023, 37, 6651−6660

Read Online

ACCESS | Metrics & More | Article Recommendations | Supporting Information

ABSTRACT: An aqueous mixture of the sterically hindered amine 2-amino-2-hydroxymethyl-1,3-propanediol (AHPD) and the cyclic diamine piperazine (PZ) is a credible CO_2 separation solvent. In this work, CO_2 absorption kinetics in AHPD/PZ mixtures was investigated in a stirred cell reactor. The solute gas CO_2 reacted in parallel with both amines AHPD and PZ. From the absorption rate measurements at 308 K, the second-order rate constant for the reaction between CO_2 and PZ was found ($k_{2,PZ}$ = 28 685 m^3 (kmol s)$^{-1}$). Several properties of this blend, such as density, viscosity, and CO_2 diffusivity and solubility, were measured. Besides, the dependency of the equilibrium CO_2 partial pressure on the loading capacity was studied in a low-pressure vapor−liquid equilibrium setup at 308 K. The highest value of CO_2 solubility in this study was 0.83 mol CO_2/mol amine, and the corresponding CO_2 partial pressure was 130 kPa. The performance of the blend AHPD/PZ (1/0.5 kmol m^{-3}) was tested in a continuous, closed-loop setup comprising an absorber (313 K) and a desorber (383 K). The efficiency of CO_2 separation from a CO_2/air mixture (12:88 v/v) was 62%, and the regeneration energy constraint was 4.21 MJ (kg CO_2)$^{-1}$. Finally, alumina catalyst was employed for faster CO_2 desorption at 368 K in a batch setup. This comprehensive study will promote the application of this candidate AHPD/PZ solvent.

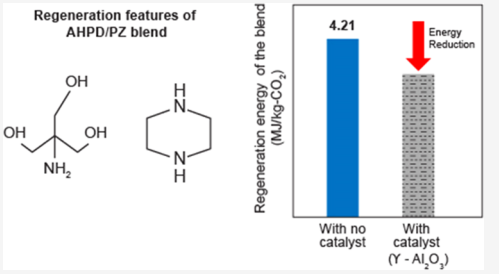

1. INTRODUCTION

The primary amine monoethanolamine (or MEA), the secondary amine diethanolamine (or DEA), and the tertiary amine methyldiethanolamine (or MDEA) are most widely used for CO_2 separation from industrial gases by the chemical absorption process. Vaidya and Kenig[1] reviewed the pathways of the reaction of CO_2 with different types of alkanolamines. In general, the usual primary and secondary amines (such as MEA and DEA) are highly reactive. However, their drawbacks are low loading capacity, high regeneration cost, and operational problems (corrosion and degradation). Contrarily, tertiary amines (e.g., MDEA) are less reactive, high loading, and easily regenerable. However, they necessitate the addition of promoters (e.g., PZ or piperazine) for improved CO_2 separation. Another class of amines, hindered amines, offers a prospective option for CO_2 capture. These amines load more CO_2 than MEA and DEA. Sartori and Savage[2] observed that steric hindrance by a bulky substituent adjacent to the amino group lowers the stability of the carbamate product. As a result, the regeneration energy constraint of sterically hindered amines (SHA) is lower than those of MEA and DEA. Overall, SHA are advantageous due to their faster reaction kinetics than tertiary amines and low regeneration cost.[3] Some of the commonly explored sterically hindered amines are 2-amino-2-methyl-1-propanol (AMP), 2-piperidineethanol (PE), 2-amino-2-methyl-1,3-propanediol (AMPD), 2-amino-2-ethyl-1,3-propandediol (AEPD), and 2-amino-2-hydroxymethyl-1,3-propanediol (AHPD). Among the aforesaid examples, AHPD is especially a promising amine. AHPD could be used as a potential solvent for acid gas removal due to its higher reactivity and CO_2 solubility.[3]

In this study, AHPD (also renowned as TRIS or THAM) is revisited. There are a few past works on AHPD in the literature, either exclusively or in blends. For example, Park et al.[4] compared CO_2 solubility in MEA and AHPD at 298 K. They found that MEA (10 wt %) loaded more CO_2 than AHPD above 4 kPa; however, the reverse was true at pressures below 4 kPa. Park et al.[5] reported solution properties, such as density and viscosity, of AHPD over wide ranges of concentrations (up to 25 wt %) and temperatures (303−343 K). The solubility of CO_2 in AHPD between 298 and 333 K was also reported by other researchers.[6−9] Among the rate promoters added to AHPD, the very reactive diamine PZ is most common. PZ reacts faster than MEA with CO_2. Upon PZ addition, both absorption kinetics and loading capacity of AHPD solutions were improved. The absorption of CO_2 into aqueous SHA/PZ mixtures was earlier investigated by a few research groups.[10−14] Bougie et al.[15] reported the physiochemical properties such as density, viscosity, solubility, and diffusivity of AHPD/PZ mixtures. In a wetted wall column,

Received: November 17, 2022
Revised: March 29, 2023
Published: April 12, 2023

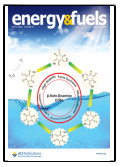

CO_2 absorption kinetics was studied and the second-order rate constant for PZ was found ($k_{2,PZ}$ = 66 450 m^3 (kmol s)$^{-1}$) at 303 K. In another work in a hollow fiber membrane contactor made of poly(tetrafluoroethylene) (PTFE), Bougie et al.[16] found that AHPD/PZ performed better than MEA.

Bougie et al.[17] found that the performance of AHPD/PZ and MEA for CO_2/N_2 separation in a flat sheet membrane contactor was comparable. Bougie and Iliuta[10] reported CO_2 solubility in AHPD/PZ blends in the 288−333 K range. Safdar et al.[18] compared CO_2 solubility in PZ (20 wt %) with that in AHPD (20 wt %) at 313 and 333 K. They found that AHPD loaded more CO_2 than PZ up to 0.8 kmol m^{-3} pressure, and the opposite was true at higher pressure. Murshid et al.[19] analyzed CO_2 solubility data in AHPD and AHPD/PZ mixtures and correlated them using the artificial neural network (ANN) model approach. Bougie and Iliuta[20] analyzed the regeneration of AHPD and AHPD/PZ mixtures. They found that the addition of a PZ activator improved the cyclic capacity of AHPD solutions.

Although CO_2 absorption in SHA is widely reported, there are relatively fewer works on the regeneration of loaded solutions. While the regenerability of AMP and AMP/PZ blends is well understood,[21−23] there are no data on AHPD and AHPD/PZ blends. Even if equilibrium and kinetic data for AHPD solutions are available, they are often not reported under identical conditions. Besides, there is disagreement due to the different methods applied for data collection and analysis. Many useful solution properties, such as density, viscosity, and CO_2 diffusivity and solubility, are scarcely reported. This work was performed to fill these aforesaid gaps in the literature.

We performed in-depth study using an AHPD/PZ blend in aqueous solutions and presented a comparison with the performance of AMP and AMP/PZ. In future, this work will aid rigorous simulation using commercial process software (e.g., ASPEN Plus), similar to the detailed analysis in a recent work of Moioli et al.[24] for applying potassium taurate. The stirred cell technique was used by us to investigate absorption kinetics in the pseudo-first-order reaction regime. Kinetic data reported in this work could be applied for developing numerical kinetics model in future. Recently, Liu et al.[25] used FEM-based COMSOL software for modeling the reactive absorption process in 1-dimethylamino-2-propanol (1DMA2P). The loading capacity of AHPD/PZ solutions was measured by us at different values of the equilibrium CO_2 partial pressure. Useful solution properties and the value of mass transfer coefficients for stirred cell were reported too. These outcomes will assist in the development of artificial neural network (ANN) models, such as those developed by Liu et al.[26] for the properties of the tertiary amine 1DMA2P, and generic artificial intelligence (AI) models similar to those of Quan et al.[27] for predicting mass transfer coefficients in the absorbers. Finally, low-temperature desorption of AHPD/PZ mixtures over the γ-Al_2O_3 catalyst was also explored to check for possible reduction in the stripping energy constraint. Metal oxides are efficient catalysts for regeneration of amine solvents.[28] The catalyst-aided desorption of AHPD-based solvents is hitherto unreported.

2. REACTION PATHWAY

SHA (such as AHPD) react with CO_2 according to a zwitterion mechanism in two steps.[29,30] This pathway also applies to the usual amines. AHPD (here, Am_1H) forms an unstable carbamate with CO_2. On the whole, this reaction is shown in eq 1

$$CO_2 + 2Am_1H \leftrightarrow Am_1COO^- + Am_1H_2^+ \quad (1)$$

Hydrolysis of the carbamate yields bicarbonate ions as follows

$$Am_1COO^- + H_2O \leftrightarrow Am_1H + HCO_3^- \quad (2)$$

The hindered amine AHPD has low tendency to form a carbamate.[3] The reaction represented by eq 3 is predominant

$$CO_2 + Am_1H + H_2O \leftrightarrow Am_1H_2^+ + HCO_3^- \quad (3)$$

Polyamines form polycarbamates with CO_2.[31] Diamine PZ (here, Am_2H) reacts according to eqs 4 and 5

$$CO_2 + Am_2H \overset{k_2, k_{-1}}{\longleftrightarrow} Am_2H^+COO^- \quad (4)$$

$$Am_2H^+COO^- + B \overset{\hat{k}_B}{\rightarrow} Am_2COO^- + BH^+ \quad (5)$$

The absorption rate (R_{CO_2}) is given by eq 6. This equation is derived by applying the steady state theory to the zwitterion. The term $\hat{k}_B$ (B) in eq 6 is attributed to base B in zwitterion deprotonation. The base B in eq 5 can be Am_2H, H_2O, and OH^-.

$$R_{CO_2} = \frac{k_2(CO_2)(\text{amine})}{1 + \frac{k_{-1}}{\hat{k}_B(B)}} \quad (6)$$

The overall rate in promoted AHPD/PZ mixtures is given by eq 7

$$R_{CO_2} = \frac{k_{2,AHPD}(CO_2)(AHPD)}{1 + \frac{k_{-1,AHPD}}{[\hat{k}_{AHPD}(AHPD) + \hat{k}_{PZ}(PZ) + \hat{k}_{H_2O}(H_2O) + \hat{k}_{OH^-}(OH^-)]}} + \frac{k_{2,PZ}(CO_2)(PZ)}{1 + \frac{k_{-1,PZ}}{[\hat{k}_{AHPD}(AHPD) + \hat{k}_{PZ}(PZ) + \hat{k}_{H_2O}(H_2O) + \hat{k}_{OH^-}(OH^-)]}} + k_{H_2O}(CO_2)(H_2O) + k_{OH^-}(CO_2)(OH^-) \quad (7)$$

The observed reaction rate constant k_{obs} (= R_{CO_2})/(CO_2)) is given by

$$k_{obs} = \frac{k_{2,AHPD}(AHPD)}{1 + \frac{k_{-1,AHPD}}{[\hat{k}_{AHPD}(AHPD) + \hat{k}_{PZ}(PZ) + \hat{k}_{H_2O}(H_2O) + \hat{k}_{OH^-}(OH^-)]}} + \frac{k_{2,PZ}(PZ)}{1 + \frac{k_{-1,PZ}}{[\hat{k}_{AHPD}(AHPD) + \hat{k}_{PZ}(PZ) + \hat{k}_{H_2O}(H_2O) + \hat{k}_{OH^-}(OH^-)]}} + k_{H_2O}(H_2O) + k_{OH^-}(OH^-) \quad (8)$$

When the contribution of CO_2 reactions with OH^- and H_2O is overlooked,[31] AND zwitterion deprotonation is instantaneous, i.e., $k_{-1,AHPD} \ll [\hat{k}_{AHPD}(AHPD) + \hat{k}_{PZ}PZ + \hat{k}_{H_2O}(H_2O) + \hat{k}_{OH^-}(OH^-)]$ and $k_{-1,PZ} \ll [\hat{k}_{AHPD}(AHPD) + \hat{k}_{PZ}(PZ) + \hat{k}_{H_2O}(H_2O) + \hat{k}_{OH^-}(OH^-)]$; it follows from eq 8 that the fast pseudo-first-order rate constant k_{obs} is obtained from the relation

$$k_{obs} = k_{2,AHPD}(AHPD) + k_{2,PZ}(PZ) \quad (9)$$

https://doi.org/10.1021/acs.energyfuels.2c03909
Energy Fuels 2023, 37, 6651−6660

3. EXPERIMENTAL SECTION

3.1. Materials. 2-Amino-2-hydroxymethyl-1,3-propanediol (AHPD) (>97% purity) and piperazine (>98% purity) were purchased from a local vendor, S.D. Fine Chemicals Pvt., Ltd., Mumbai. Another dealer, Molychem Pvt., Ltd., Mumbai, provided methanol (analytical reagent grade), sodium hydroxide, hydrochloric acid (32%), and alumina (Al_2O_3) catalyst. Cylinders containing CO_2, N_2 with purity > 99.95%, and nitrous oxide (N_2O) were purchased from Inox Air Products Ltd., Mumbai.

3.2. Methodology. *3.2.1. Estimation of Solution Properties.* The knowledge of solution density and viscosity is vital for determining other physicochemical properties such as diffusivity and gas solubility. The density and viscosity of the AHPD/PZ blend were measured at 308 K using a density meter (DMA 5000, Anton Parr) and Oswald's viscometer, respectively. Trials were performed using BSS number 3 J-SIL borosilicate glass.

3.2.2. Stirred Cell Kinetics. The trials on kinetics were carried out in a jacketed stirred cell with a volume of 1.45 L. The flat gas–liquid interface had a surface area of 4.3×10^{-3} m^2. To remove air and ensure an inert environment, N_2 gas was used before each trial. After that, the reactor was evacuated and 400 mL of amine solution was charged inside. Pure CO_2 was introduced thereafter from the gas reservoir. The stirring speeds in the gas and liquid were 1000 and 60 rpm. The pressure reduced with time due to absorption, and it was adequate to know this pressure history for finding the absorption rates at 308 K.[32] By repeating a few trials, the error in measuring rates (2%) was determined. We anticipated that there was no resistance to the mass transfer of CO_2 in the gas phase because the partial pressure of inert gas was low and agitation was intense. The liquid stirring speed (n) was increased from 60 to 100 rpm, but the absorption rates remained constant. It was thus evident that the value of k_L had no effect on the rates.

3.2.3. Vapor–Liquid Equilibrium (VLE) Measurements. In a past work, we described the setup used for VLE trials.[33] In this setup, an equilibrium cell (capacity 250 mL) was immersed in a water bath maintained at 308 K. A magnetic stirrer (Remi Instruments, Mumbai) and conductivity probe were provided for this cell (EQ-610, pH meter, Equiptronics, Mumbai). The inlet and exit ports of the cell were linked to a saturator and gas reservoir (also immersed in the bath). The amine solution (250 mL) was loaded with CO_2 and charged inside the cell. To ensure gas flow inside the apparatus, a blower was used. The method of titration was used to analyze both phases after equilibrium was reached. An aqueous solution of sodium hydroxide was injected inside the gas reservoir using a syringe. To ensure that all CO_2 was absorbed, the reservoir was vigorously shaken and left undisturbed for 48 h. After that, the caustic solution was titrated against HCl using 2–3 drops of phenolphthalein indicator. The excess NaOH and carbonate ions in the sample were converted to bicarbonate during this titration to the first equivalence point. In the second step of titration, methyl orange was used as an indicator to convert all bicarbonates to carbonic acid.[34] The calculated carbonate concentration was converted into moles, and the equilibrium CO_2 partial pressure ($P^*_{CO_2}$) was determined using the ideal gas equation. The method of titration was also used to determine the CO_2 content in the liquid phase: the pH of methanol was adjusted to 11 using caustic solution. To this, a known weight (2.5 g) of a sample of CO_2-loaded amine solution was added in a vial. This mixture was then titrated with sodium hydroxide to pH = 11. The loading capacity (α) was calculated using the second volume of NaOH.[35]

3.2.4. Heat Duty Estimation Using a Bench Scale Setup. A closed-loop cyclic setup comprising a CO_2 absorption column and a desorption column was used in all trials. A detailed description of this setup was given in our previous work.[23] In this setup, the CO_2-rich solvent stream exiting from the bottom of the absorber and the hot CO_2-lean solvent stream exiting from the bottom of the stripper were brought into countercurrent contact for improved heat transfer. The CO_2-rich solvent stream, which enters the stripper at the top stage, is partially vaporized as a result of the heat exchange. The solvent flows down the stripper column and transfers CO_2 to the outlet, while the vapors of amine and water condense and flow down the stripper. The absorber and desorber were kept at 313 and 383 K, respectively. The pressure in the system was maintained at 0.2 MPa. The gas flow rate (G) was varied between 0.36 and 0.78 $m^3\ h^{-1}$, while the liquid solvent was circulated at a flow rate of L = 6 L h^{-1}. The CO_2 concentration in the gas entering the absorber was fixed (12 mol %). The heat capacity of the amine solution was assumed to be constant throughout the column length. After reaching steady state, the temperatures in both columns were measured. The liquid samples were collected at regular intervals from the sampling ports, while the gaseous samples were taken from the top of the absorber. The liquid sample was analyzed using the CO_2 titration method described by Artanto et al.[35] to determine the CO_2 loading of the absorbent (α). The gaseous sample was analyzed using gas chromatography in which a thermal conductivity detector was used. Hydrogen was the carrier gas flowing through HayeSep-DB column (maximum temperature 563 K). The amine concentration was regularly checked. The experiment was continued for up to 15 h; by then, there was no significant change in the cyclic loading of the solution.

The regeneration energy (Q_{Reg}) is typically composed of the heat of desorption (Q_{Des}), the sensible heat (Q_{Sens}), and the heat of vaporization (Q_{Vap}). The heat of desorption (Q_{Des}) is the heat required to break the chemical bond between amine and CO_2, and it is calculated using the formula

$$Q_{Des} = \frac{\Delta h_{abs}}{M_{CO_2}} \tag{10}$$

Here, M_{CO_2} and Δh_{abs} denote the molecular weight of CO_2 (g mol^{-1}) and the heat of absorption (kJ mol^{-1}), respectively. An enthalpy change (Δh_{abs}, kJ $(mol\ CO_2)^{-1}$) occurs when gaseous CO_2 is dissolved in the amine solution. This value can be determined experimentally using a reaction calorimeter or with the help of vapor–liquid equilibrium (VLE) data. Jiang et al.[36] obtained the Δh_{abs} value through VLE measurements, and it agreed with the value obtained through comprehensive Aspen modeling. This indicates the validity and reliability of the VLE data to predict the heat of CO_2 reaction

$$\frac{d(\ln P^*_{CO_2})}{d\left(\frac{1}{T}\right)} = \frac{\Delta h_{abs}}{R} \tag{11}$$

In eq 11, Δh_{abs} is the heat of CO_2 absorption (J mol^{-1}), $P^*_{CO_2}$ is the equilibrium CO_2 partial pressure, T is the temperature (K), and R is the universal gas constant (J $(mol\ K)^{-1}$). The Δh_{abs} value can be obtained from the slope of the plot between ln $P^*_{CO_2}$ and $1/T$ using a set of $P^*_{CO_2}$ and T data of similar CO_2 solubility.[37] VLE data for the AHPD/PZ blend, reported in a past work,[10] were used here. Using eq 11, Δh_{abs} for AHPD/PZ was found to be 61 149 kJ mol^{-1}.

Sensible heat (Q_{sens}) is found from the relation between the specific heat capacity C_P (kJ $(mol\ K)^{-1}$) and the temperature approach (ΔK), viz., the difference between the temperature of the lean solution leaving the bottom of the desorber and rich solution entering the top of the desorber[37]

$$Q_{Sens} = \frac{C_p \Delta T}{(\alpha_{rich} - \alpha_{lean}) x_{amine} M_{CO_2}} \tag{12}$$

Here, x_{amine} denotes the mole fraction of amine in the liquid.

The heat of vaporization (Q_{Vap}) depends upon the concentration of water in the amine mixture and is represented by

$$Q_{Vap} = \frac{p_{H_2O}}{p_{CO_2}} \frac{\Delta h_{vap}}{M_{CO_2}} \tag{13}$$

In eq 13, Δh_{vap} is the latent heat of vaporization of water (kJ mol^{-1}). The partial pressures (kPa) of water vapor and CO_2 leaving the stripper are denoted by P_{H_2O} and P_{CO_2}, respectively. Their values can be calculated by the Antoine equation and Dalton's law.[23] A stripper pressure of 200 kPa and regeneration temperature of 383 K

https://doi.org/10.1021/acs.energyfuels.2c03909
Energy Fuels 2023, 37, 6651–6660

were used for AHPD/PZ regeneration trials. The regeneration energy (Q_{Reg}) is determined by the summation of eqs 10, 12, and 13, i.e.,

$$Q_{Reg} = Q_{Des} + Q_{Sens} + Q_{Vap} \quad (14)$$

3.2.5. Catalytic Desorption. Catalyst-aided amine regeneration is a potential method for improving CO_2 desorption, thereby reducing the solvent regeneration cost. Metal oxides are efficient catalysts for the regeneration of CO_2-rich amine solutions. In this work, the solid acid catalyst alumina was used for the regeneration of amine-based solvents at T = 368 K. An Al_2O_3 catalyst was especially chosen for its electron acceptor and proton donation capabilities. These acidic properties are specifically desirable in CO_2 desorption because they have the potential to reduce the heat required for the deprotonation and breakdown of carbamate and bicarbonate. The setup, which was described in our recent work,[38] comprised a 500 mL three-neck round-bottom desorption flask immersed inside an oil bath. A magnetic stirrer was used (Remi Instruments, Mumbai). In every trial, 200 mL of CO_2-loaded sample was taken. A condenser was connected to a neck of the desorption flask to prevent the loss of amine and water vapors. The second neck was equipped with a thermometer for measuring the temperature of the amine solution. The final neck was fitted with a stopper and used to collect samples of the amine solution. The desorption flask was heated to 368 K. This setup was well-insulated to prevent heat loss. Both catalytic and noncatalytic desorption of AHPD/PZ mixtures was studied. The chosen catalyst/solvent ratio was 1:80.[28,39] The reaction was conducted for 90 min. The concentration of CO_2 was determined at regular time intervals by the titration method.[35] An auto titrator was used (877 Titrino Plus Auto titrator, Metrohm India Private Limited, Bangalore).

3.2.6. Characterization by Attenuated Total Reflectance–Fourier Transform Infrared (ATR-FTIR) Spectroscopy. The samples of the unused AHPD/PZ blend, CO_2-loaded mixture, and desorbed solution were characterized using attenuated total reflectance–Fourier transform infrared (ATR-FTIR) spectroscopy. PerkinElmer's Frontier FTIR spectrometer, equipped with a reflection accessory, was used to record spectra at ambient temperature in the 4000–450 cm^{-1} range.

4. RESULTS AND DISCUSSION

4.1. Determination of Physical Properties. The density and viscosity of AHPD/PZ mixtures were measured at 308 K, and these values are shown in the Supporting Information in Table S1. The N_2O analogy was used to determine the solubility and diffusivity of CO_2 in the AHPD/PZ blend because N_2O is a nonreactive gas whose molecular volume and electronic configuration are similar to those of CO_2.[40] Thus, it can be used to estimate the properties of reactive CO_2 in the amine solution. The N_2O analogy method suggests that the ratio of the solubilities of CO_2 and N_2O remains constant for aqueous amines

$$(\text{solubility of } CO_2) = C_1(\text{solubility of } N_2O) \quad (15)$$

where C_1 is given by

$$C_1 = \frac{(\text{solubility of } CO_2 \text{ in water})}{(\text{solubility of } N_2O \text{ in water})} \quad (16)$$

The stirred cell was used for determining the solubility of N_2O in amine solutions (H_{N_2O}). The measurement technique was corroborated by studying the physical absorption of CO_2 in water. The solubility of CO_2 in water at T = 308 K was found to be 2.7 × 10^{-4} kmol (m^3 kPa)$^{-1}$. This value was substituted in eq 16. The measured values of viscosity were used to determine the diffusivity in the solution using the modified Stokes–Einstein relation.[32] The values of CO_2 diffusivity in AHPD/PZ mixtures are shown in the Supporting Information in Table S1. It was observed that the solubility of CO_2 in AHPD/PZ mixtures (AHPD = 1 kmol m^{-3}) at 308 K did not vary significantly even when the molarity of PZ was varied in the 0.25–1 kmol m^{-3} range. This trend was also observed earlier by Sun et al.[12] for the blend AMP/PZ.

4.2. Evaluation of Liquid-Side Mass Transfer Coefficient (k_L). A procedure for estimating the liquid-side mass transfer coefficient k_L in a stirred cell reactor was previously reported by Littel et al.[41] For the case of physical absorption in a stirred cell reactor, a solute mass balance for both the gas and liquid phases results in the following correlation

$$\ln\left[\frac{P(t) - P_{final}}{P_{initial} - P_{final}}\right] = -\left[\frac{(\hat{m}V_L) + V_G}{V_L V_G}\right]k_L A t \quad (17)$$

The physical absorption of CO_2 in water at 308 K was studied and the pressure drop due to absorption was recorded. A plot of $\ln\left[\frac{P(t) - P_{final}}{P_{initial} - P_{final}}\right]$ vs time was used to estimate the value of k_L.[32,33] The slope of this graph equals $-\left[\frac{(\hat{m}V_L) + V_G}{V_L V_G}\right]k_L A$. The value of k_L at a stirring speed of 60 rpm in water was determined (5 × 10^{-5} m s^{-1}). This value is comparable with those seen in stirred cell reactors.[32]

4.3. Kinetics of the AHPD/PZ Blend. The procedure for kinetics measurement was discussed in our previous work.[32] For the chosen blend, the absorption rate is estimated using eq 18

$$R_{CO_2} = k_L(CO_2)E \quad (18)$$

Here, (CO_2) is the saturation concentration of CO_2 and $k_L(CO_2)$ is the absorption rate for the diffusion-controlled regime. The Hatta number is a useful parameter that provides the value for the enhancement factor (E) when the reaction is fast

$$Ha = \frac{\sqrt{D_{CO_2}k_{obs}}}{k_L} \quad (19)$$

It is necessary that the following condition should be valid: $10 < Ha \ll (E_i - 1)$. Here, E_i is the instantaneous enhancement factor, whose value as per the film theory is

$$E_i = 1 + \left[\frac{(AmH)}{z(CO_2)}\frac{D_{AmH}}{D_{CO_2}}\right] \quad (20)$$

D_{AmH} denotes the diffusivity of AmH in liquid, whereas z denotes the stoichiometric reaction coefficient. It follows from eqs 18 and 19 that the rate is given by

$$R_{CO_2} = P_{CO_2}H_{CO_2}\sqrt{D_{CO_2}k_{obs}} \quad (21)$$

Here, k_{obs} is given by eq 9. Substituting the value of k_{obs} from eq 9, eq 21 is rewritten as

$$R_{CO_2} = P_{CO_2}H_{CO_2}\sqrt{D_{CO_2}[k_{2,AHPD}(AHPD) + k_{2,PZ}(PZ)]} \quad (22)$$

In fact, two parallel reactions of CO_2 with AHPD and PZ constitute the whole reaction. The agitation speed and, thus, k_L does not influence the absorption rate if the reaction is a fast pseudo-first-order reaction. Between 60 and 120 rpm, the absorption rate was almost constant. Thus, the fast pseudo-first-order regime was verified. We used a speed of 60 rpm in all runs thereafter. At 308 K, we measured rates in an AHPD/PZ blend (1/0.5 kmol m^{-3}) at different partial pressures of

https://doi.org/10.1021/acs.energyfuels.2c03909
Energy Fuels 2023, 37, 6651–6660

CO_2. It is clear from Figure 1 that the absorption rate increased linearly with CO_2 partial pressure. This behavior is

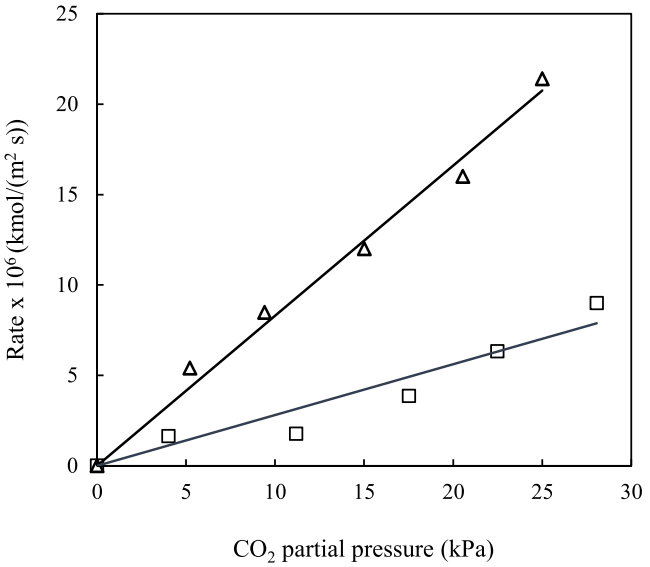

Figure 1. Plot of R_{CO_2} vs CO_2 partial pressure at 308 K. (Δ) AHPD/PZ (1/0.5 kmol m^{-3}) and (□) AHPD (1 kmol m^{-3}).

identical to the trend shown in past works on alkanolamine blends.[31,32] The rates in 1/0.5 kmol m^{-3} AHPD/PZ mixtures were higher than those in 1 kmol m^{-3} AHPD (see Figure 1). When promoter was added to aqueous AHPD solution, the CO_2 absorption rates improved. When both AHPD and PZ are present, the zwitterion $Am_2H^+COO^-$ transfers CO_2 to Am_1H (viz. AHPD) according to eq 23 and Am_2H (here, PZ) is regenerated

$$Am_2H^+COO^- + Am_1H \leftrightarrow Am_1H^+COO^- + Am_2H \quad (23)$$

In this way, PZ influences the absorption process and improves the rate. In Table 1, the CO_2 absorption rates at various PZ concentrations are represented. The respective values of the mass fraction of amines are also shown in Table 1. Using the D_{CO_2} and H_{CO_2} values at 308 K, the value of k_{obs} was calculated (see Table 1). When PZ molarity is raised, k_{obs} increases too.

At T = 308 K and P_{CO_2} = 5 kPa, the rate in aqueous AHPD (1.5 kmol m^{-3}) was 1.2 × 10^{-6} kmol (m^2 s)$^{-1}$. It increased to 5.4 × 10^{-6} kmol (m^2 s)$^{-1}$ in the AHPD/PZ blend (1/0.5 kmol m^{-3}). Bougie and Iliuta[3] reported the value of $k_{2,AHPD}$ (389 m^3 (kmol s)$^{-1}$) at 308 K. By substituting this value in eq 9, the second-order rate constant $k_{2,PZ}$ for the AHPD/PZ blend (1/0.5 kmol m^{-3}) was found to be 28 686 m^3 (kmol s)$^{-1}$. This value is fairly close to that reported by Konduru et al.[42] (24 450 m^3 (kmol s)$^{-1}$). Bougie et al.[15] reported a higher value of $k_{2,PZ}$ in the AHPD/PZ blend (66 450 m^3 (kmol s)$^{-1}$) at 308 K. This difference in the value of $k_{2,PZ}$ is because different model contactors were used for measuring rates and solution properties. Table 2 shows the values of the second-order rate constant for PZ in different SHA/PZ blends, viz., AMPD/PZ,[14] AHPD/HEPZ[43] (HEPZ denotes *N*-(2-hydroxyethyl)-piperazine), and AHPD/PZ.[15] The effects of promoter concentration on k_{obs} in different amine blends are shown in Figure 2. Clearly, the k_{obs} values for this work are in good agreement with those reported for the other SHA/promoter mixtures.[12−15,43] Since the rates did not significantly improve above 0.5 kmol m^{-3} PZ concentration, the curve in Figure 2 gradually flattened. It is evident that the chosen blend AHPD/PZ is very attractive for bulk CO_2 removal.

4.4. VLE Results. To obtain the data of partial pressure of CO_2 at equilibrium ($P^*_{CO_2}$) vs the loading capacity (∝) of AHPD/PZ solutions (1/0.5 kmol m^{-3}), VLE trials were carried out at 308 K. The results for CO_2 partial pressure in the 5−130 kPa range are represented in Figure 3. A rise in the loading capacity from 0.09 to 0.83 mol CO_2/mol amine was observed; correspondingly, $P^*_{CO_2}$ increased from 5 to 130 kPa. The equilibrium solubility data for AHPD/PZ reported in this work were compared with the data reported by Bougie and Iliuta[10] for AHPD/PZ (1/0.5 kmol m^{-3}) at 313 K. Our data were also compared with the data for 0.83 kmol m^{-3} aqueous AHPD without a promoter[5] (see Figure 3). The tendencies of unpromoted and promoted AHPD solutions are evident. The following relation between $P^*_{CO_2}$ and ∝ (range: 0.09−0.83 mol CO_2/mol amine) for AHPD/PZ (1/0.5 kmol m^{-3}) mixtures was established based on this study

$$\log(P^*_{CO_2}) = -4.32 + 83.86 \propto +86.17 \propto^2 +4.57\propto^3 \quad (24)$$

4.5. Study of Amine Regeneration. The effect of changing L/G ratios on the cyclic loading capacity and % CO_2 removal was studied in the 7.69−16.6 L m^{-3} range. The results for AHPD-PZ (1/0.5 kmol m^{-3}) blend are represented in Table 3. The cyclic capacity increased from 0.03 to 0.54 mol mol^{-1} as the L/G ratio increased from 7.69 to 16.6 L m^{-3}. The respective values of % CO_2 removal increased from 11 to 62%.

The effect of L/G ratios on Q_{Reg} is shown in Figure 4. When the L/G ratio increased from 7.69 to 16.6 L m^{-3}, Q_{Reg} decreased from 13 to 4.21 MJ (kg CO_2)$^{-1}$. The increase in L/G ratios and, thus, loading capacity is advantageous for lower energy requirements. In Table 4, values of the regeneration energy reported in the literature for various amines are represented. Artanto et al.[21] reported Q_{Reg} values of 4.3 (for MEA) and 4.9 MJ kg^{-1} (for AMP/PZ), while Singh et al.[22] reported that the value for AMP/HMDA was 4.41 MJ kg^{-1}. Muchan et al.[44] reported a high value for MEA (16.92 MJ kg^{-1}). In our previous work, Patil et al.[23] reported that AMP/PZ exhibits a Q_{Reg} value of 3.65 MJ kg^{-1}. The present work suggests a value of 4.21 MJ kg^{-1} for the AHPD/PZ blend. This

Table 1. Kinetic Characteristics of CO_2 Absorption into AHPD/PZ Aqueous Blend at 308 K

(AHPD) + (PZ) (kmol m^{-3})	mass fraction of amine	D_{CO_2} × 10^9 (m^2 s^{-1})	H_{CO_2} × 10^4 (kmol (m^3 kPa)$^{-1}$)	P_{CO_2} (kPa)	R_{CO_2} × 10^6 (kmol (m^2 s)$^{-1}$)	*Ha*	k_{obs} (s^{-1})	E_i
1.0 + 0.25	0.14	1.63	2.40	5	3.96	66	6681	209
1.0 + 0.50	0.16	1.61	2.31	4.8	5.4	97	14 732	452
1.0 + 0.75	0.18	1.59	2.29	5	5.8	101	16 138	656
1.0 + 1.0	0.20	1.57	2.34	5	6.03	103	16 919	856

https://doi.org/10.1021/acs.energyfuels.2c03909
Energy Fuels 2023, 37, 6651−6660

Table 2. Kinetic Studies on the CO_2−Aqueous PZ Reaction System

reaction system	temperature (K)	model laboratory contactor	rate constant (m^3 (kmol s)$^{-1}$)	refs
AMPD/PZ	298	stopped flow apparatus	23 319	Gordesli et al.[14]
AHPD/N-HEPZ	298	stopped flow apparatus	12 971	Ume et al.[13]
AHPD/PZ	303	wetted wall column	66 450	Bougie et al.[15]
AHPD/PZ	308	stirred cell reactor	28 686	this study

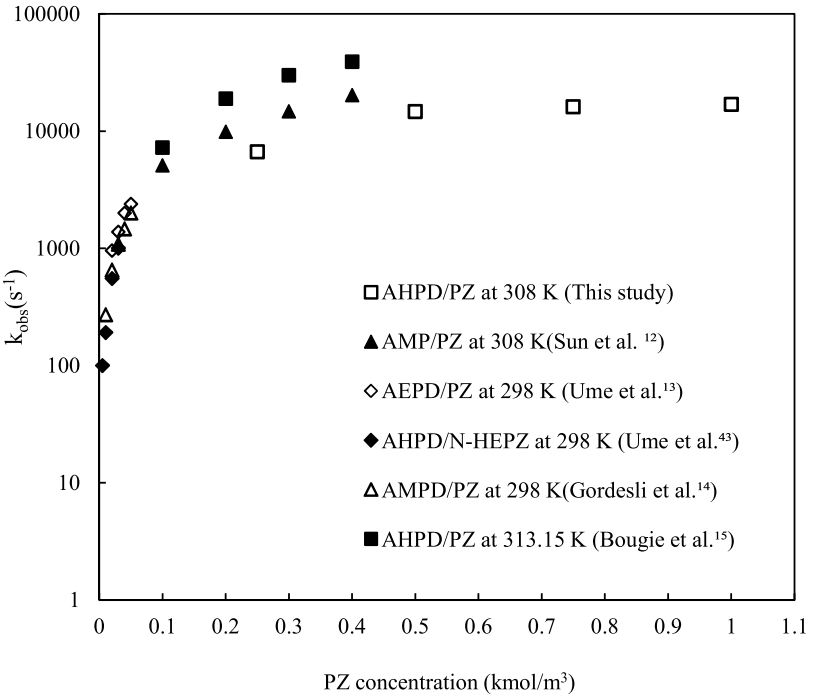

Figure 2. Effect of promoter on k_{obs} in different amine blends.

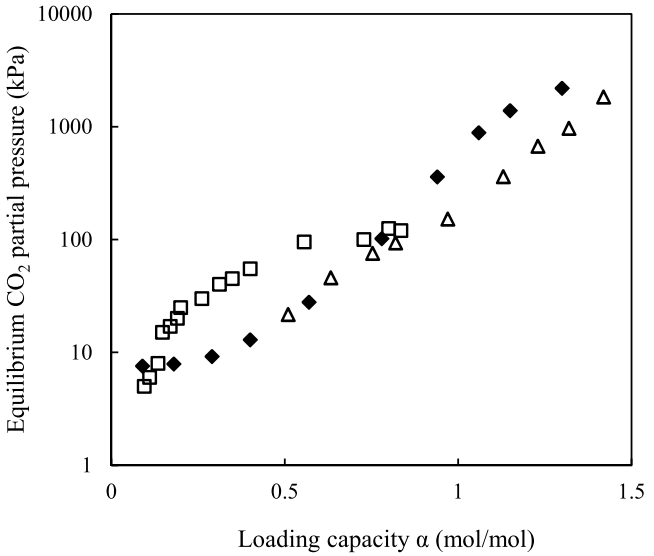

Figure 3. Equilibrium CO_2 partial pressure vs loading capacity. (□) AHPD/PZ (1/0.5 kmol m^{-3}) at 308 K (this study), (♦) AHPD/PZ (1/0.5 kmol m^{-3}) at 313 K (Bougie et al.[10]), and (Δ) aqueous AHPD (0.83 kmol m^{-3}) at 313 K (Park et al.[5]).

value can be further improved, for example, by working with concentrated AHPD/PZ mixtures.

4.6. Catalytic Desorption of CO_2-Loaded AHPD/PZ Mixtures. The addition of a catalyst is beneficial for the regeneration process because it results in desorption of greater amounts of CO_2, improved rates of CO_2 desorption, and increased cyclic loading capacity of the absorbent.[28] Catalysts provide alternative low-energy pathway, thereby enabling CO_2 desorption at lower temperatures. For instance, catalysts interact with the carbamate, alter the configuration of the N-atom, and weaken the C−N bond in the carbamate.

The effect of the Lewis acid catalyst Al_2O_3 on the desorption of CO_2-loaded solutions of AHPD/PZ (1/0.5 kmol m^{-3}) was studied. The variation in CO_2 loading of solution with time is shown in Figure 5. Clearly, the extent of desorption for the catalytic process is higher. A relevant parameter for this study is the cyclic capacity of the solution, which is defined as the difference between the initial CO_2-rich loading at the start of the experiment and the final minimum CO_2 loading when the experiment ends. The cyclic capacity was determined by using eq 25

$$\text{cyclic loading} = (\alpha_{\text{rich}} - \alpha_{\text{lean}}) \tag{25}$$

Furthermore, the cyclic capacity was used to calculate the rate of desorption of CO_2 from the amine solution. The rate of desorption of CO_2 describes the rate of transfer of CO_2 from the liquid phase (amine solution) to the gas phase. A solution with a higher desorption rate results in a lower heat duty. The rate of desorption was calculated using eq 26

$$r = \frac{(\alpha_{\text{rich}} - \alpha_{\text{lean}})}{t} = \frac{Q_{\text{Cyc}}}{t} \tag{26}$$

https://doi.org/10.1021/acs.energyfuels.2c03909
Energy Fuels 2023, 37, 6651−6660

Table 3. Influence of L/G Ratio on the Loading Capacity of AHPD/PZ (1/0.5 kmol m^{-3}) and % CO_2 Removal at Absorber Temperature = 313 K and Desorber Temperature = 383 K

solvent flow rate (L) (L h^{-1})	gas flow rate (G) (m^3 h^{-1})	L/G (L m^{-3})	α_{rich} (mol mol^{-1})	α_{lean} (mol mol^{-1})	cyclic loading (mol mol^{-1})	CO_2 removal (%)
6	0.78	7.69	0.7	0.64	0.03	11
	0.6	10	0.7	0.45	0.25	22.4
	0.48	12.5	0.8	0.4	0.4	51.2
	0.36	16.6	0.92	0.38	0.54	62

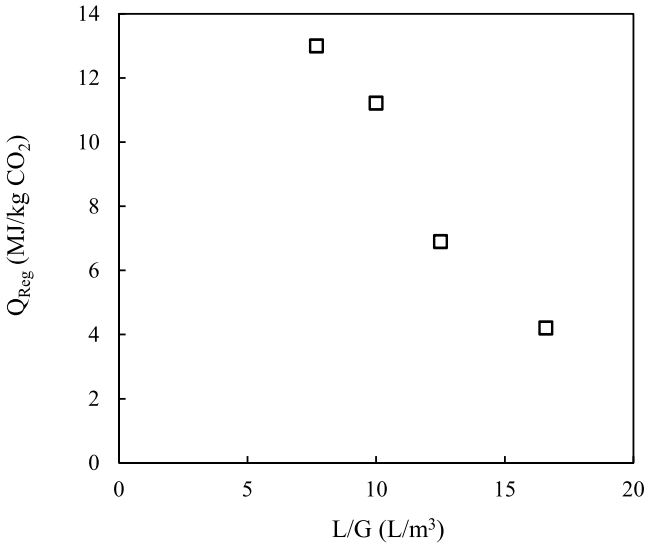

Figure 4. Influence of L/G ratio on regeneration energy for AHPD/PZ (1/0.5 kmol m^{-3}) blend.

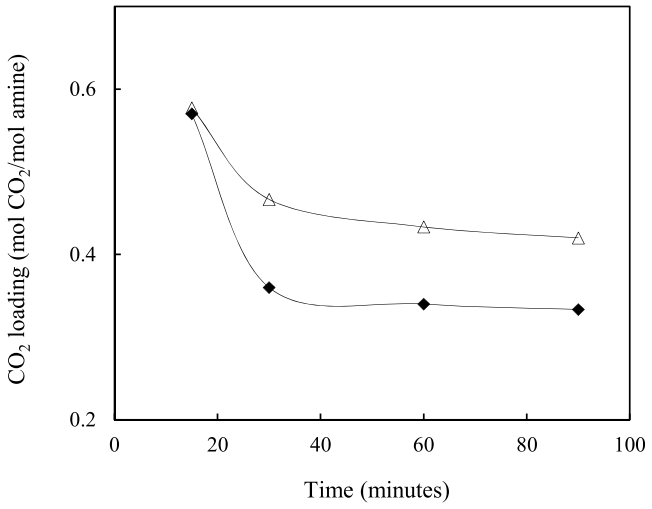

Figure 5. CO_2 loading with and without catalyst as a function of time at 368 K. (Δ) AHPD/PZ (1/0.5 kmol m^{-3}) without catalyst, and (♦) AHPD/PZ (1/0.5 kmol m^{-3}) with catalyst.

where r is the rate of desorption, α_{rich} and α_{lean} (mol CO_2/mol amine) are the values of CO_2 loading of the AHPD/PZ solution before and after the experiment, respectively, and t is the duration of the experiments in hours.[28] The values of cyclic capacity and desorption rate for AHPD/PZ (1/0.5 kmol m^{-3}) blends with and without catalyst at 368 K after 90 min of desorption are shown in Table 5. The cyclic capacity of the catalytic solution (AHPD/PZ-Al_2O_3) was higher than that of the noncatalytic (AHPD/PZ) solution. The rate of desorption improved from 0.1 (noncatalytic process) to 0.18 mol CO_2/(mol amine h) (catalytic desorption) because more CO_2 was released from the catalytic solutions. A solvent with a higher cyclic capacity is highly advantageous because it requires lower solvent circulation rates and a shorter column for regeneration. With the help of a catalyst for desorption, the stripping temperature could be lowered from 383 to 368 K. The results obtained are promising and suggest reduced values of Q_{Reg}.

4.7. Analysis by ATR-FTIR Spectroscopy. The IR spectra for the fresh AHPD/PZ blend (black line), CO_2-loaded solution (red line), and desorbed solution (blue line) are represented in Figure 6. The O−H stretching of H_2O between 3200 and 3700 cm^{-1} is evident. For the fresh solution (black line), the vibration mode at 1642 cm^{-1} was attributed to the N−H bond. Besides, C−N and C−O stretching modes were seen at 1076 and 1033 cm^{-1}, respectively. The main peak at 1464 cm^{-1} was possibly due to the asymmetric $-CH_3$ group. After amine protonation (red line) C−N and C−O stretching modes were seen at 1069 and 1024 cm^{-1}, respectively. At higher CO_2 loading, peaks for bicarbonate species were evident at 1288 and 1289 cm^{-1} (C−OH bending). Carbamate peaks seen at 1534, 1471, and 1371 cm^{-1} were assigned to COO

Table 4. Comparison of the Regeneration Energy Value of This Work with the Literature

amine	CO_2 composition at the inlet of the absorber	regeneration temperature (K)	loading (mol mol^{-1})	regeneration energy (MJ $(kg\ CO_2)^{-1}$)	refs
MEA (5.1 kmol m^{-3})	11−13	385	0.18	4.3	Artanto et al.[21]
AMP/PZ (2.8/0.6 kmol m^{-3})	11−13	383	0.14	4.9	Artanto et al.[21]
AMP/HMDA (3/1 kmol m^{-3})	10	395	0.42	4.41	Singh et al.[22]
MEA (2 kmol m^{-3})	15	363	0.5	16.92	Muchan et al.[44]
AMP/PZ (2.5/0.5 kmol m^{-3})	12	383	0.4	3.65	Patil et al.[23]
AHPD/PZ (1/0.5 kmol m^{-3})	12	383	0.54	4.21	this study

https://doi.org/10.1021/acs.energyfuels.2c03909
Energy Fuels 2023, 37, 6651−6660

Table 5. CO_2-Desorption Performance of AHPD/PZ (1/0.5 kmol m^{-3}) Blend with and without Catalyst at 368 K

	α_{rich} (mol CO_2/mol AHPD)	α_{lean} (mol CO_2/mol AHPD)	Q_{Cyc} (mol CO_2/mol AHPD)	r (mol CO_2/(mol amine h))
AHPD/PZ	0.57	0.42	0.15	0.10
AHPD/PZ-Al_2O_3	0.6	0.33	0.27	0.18

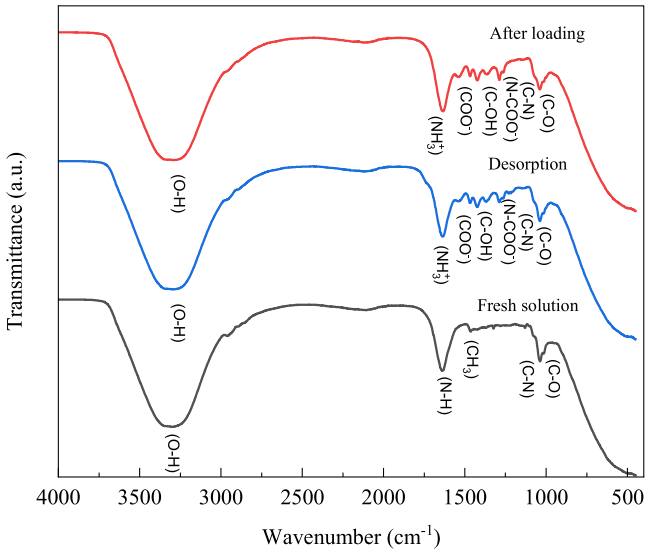

Figure 6. Infrared spectra of the liquid phase of fresh AHPD/PZ solution (black line), solution after loading (red line), and solution after desorption (blue line).

asymmetric and symmetric stretching and N−COO stretching vibrations, respectively.[45,46] For the case of desorption (blue line), the stretching of C−N and C−O decreased from 1076 to 1072 and 1033 to 1030 cm^{-1}, respectively. During desorption, little shifts in all peaks (when compared to the loaded solution) were observed. Overall, these outcomes supported our aforesaid results.

5. CONCLUSIONS

AHPD/PZ mixtures represent a candidate CO_2-capturing solvent with high loading capacity and reactivity. Here, we investigated CO_2 absorption kinetics in the AHPD/PZ blend in aqueous medium in a stirred cell reactor. At 308 K, absorption rates were measured in the fast pseudo-first-order reaction regime. The rates were higher when molarity of PZ in solutions was raised. The value of the rate constant for PZ was found to be 28 685 m^3 (kmol s)$^{-1}$. These data will be useful in future for developing a comprehensive numerical kinetics model. We measured physicochemical properties of the proposed blend, namely, density, viscosity, diffusivity, and solubility. We measured the liquid-side mass transfer coefficient (0.005 cm s^{-1}). In future, data on solution properties and mass transfer coefficients may be modeled using artificial neural networks. We also measured equilibrium CO_2 solubility at 308 K, and the results were encouraging. The highest value of CO_2 solubility in this study was 0.83 mol CO_2/mol amine, and the corresponding CO_2 partial pressure was 130 kPa. Besides, continuous absorption−desorption trials were performed in a setup. The absorber and desorber temperatures were 313 and 383 K. AHPD and PZ molarity were 1 and 0.5 kmol m^{-3}, respectively. The gas phase was a mixture of CO_2 (12%) and air. Around 62% CO_2 was absorbed. The regeneration energy required was 4.21 MJ (kg CO_2)$^{-1}$. Catalyst-aided amine desorption was explored. Alumina catalyst was used for faster CO_2 desorption at 368 K in a batch setup. Finally, FTIR characterization of blends was in line with the outcomes. While our results are encouraging, the performance of concentrated AHPD/PZ mixtures is not yet reported. More work in this direction will be useful. Nevertheless, this work will draw attention to this promising solvent.

ASSOCIATED CONTENT

Supporting Information

The Supporting Information is available free of charge at https://pubs.acs.org/doi/10.1021/acs.energyfuels.2c03909.

Properties of blends of sterically hindered amines (PDF)

AUTHOR INFORMATION

Corresponding Author

Prakash D. Vaidya − *Department of Chemical Engineering, Institute of Chemical Technology, Mumbai 400019, India;* orcid.org/0000-0001-5061-9635; Phone: +91 22 3361 2014; Email: pd.vaidya@ictmumbai.edu.in; Fax: +91 22 3361 1020

Authors

Shaurya Mohan − *Department of Chemical Engineering, Institute of Chemical Technology, Mumbai 400019, India*

Namrata Upreti − *Department of Chemical Engineering, Institute of Chemical Technology, Mumbai 400019, India*

Complete contact information is available at: https://pubs.acs.org/10.1021/acs.energyfuels.2c03909

Notes

The authors declare no competing financial interest.

ACKNOWLEDGMENTS

Acknowledgments are due to Centre for High Technology, Ministry of Petroleum and Natural Gas, Government of India, for financial assistance.

NOMENCLATURE

A = interfacial area, m^2
AmH = amine
(AmH) = concentration of amine, kmol m^{-3}
C_{amine} = concentration of amine, kmol m^{-3}
C_p = heat capacity of the solution, kJ (kg K)$^{-1}$
CO_2 = saturation concentration of CO_2, kmol m^{-3}
D_{AmH} = diffusivity of amine in liquid, m^2 s^{-1}
D_{CO_2} = diffusivity of CO_2 in liquid, m^2 s^{-1}
E_i = enhancement factor for an instantaneous reaction
G = gas flow rate, m^3 h^{-1}
Ha = Hatta number
H_{CO_2} = solubility of CO_2, kmol (m^3 kPa)$^{-1}$
Δh_{abs} = heat of absorption of CO_2, kJ mol^{-1}
Δh_{vap} = latent heat of vaporization of water, kJ mol^{-1}
(H_2O) = concentration of water, kmol m^{-3}
k_2 = forward rate constant for reaction between CO_2 and amine, m^3 (kmol s)$^{-1}$

https://doi.org/10.1021/acs.energyfuels.2c03909
Energy Fuels 2023, 37, 6651−6660

k_{-1} = reverse rate constant for reaction between CO_2 and amine, m^3 (kmol s)$^{-1}$
k_L = liquid-side mass transfer coefficient, m s^{-1}
$\hat{k}_{AHPD}$ = deprotonation constant for AHPD
$\hat{k}_{H_2O}$ = deprotonation constant for water
$\hat{k}_{OH^-}$ = deprotonation constant for OH^-
$\hat{k}_{PZ}$ = deprotonation constant for PZ
L = liquid flow rate, L h^{-1}
$\hat{m}$ = dimensionless solubility, mol mol^{-1}
M_{CO_2} = molecular weight of CO_2, g mol^{-1}
(OH^-) = hydroxyl ion concentration, kmol m^{-3}
P_{final} = final partial pressure of solute gas, kPa
$P_{initial}$ = initial partial pressure of solute gas, kPa
$P(t)$ = partial pressure of solute gas at time t, kPa
P_{CO_2} = partial pressure of CO_2, kPa
P_{H_2O} = partial pressure of water, kPa
Q_{Des} = heat of desorption, MJ (kg CO_2)$^{-1}$
Q_{Reg} = heat of regeneration of solvent, MJ (kg CO_2)$^{-1}$
Q_{Sens} = sensible heat, MJ (kg CO_2)$^{-1}$
Q_{Vap} = heat of vaporization, MJ (kg CO_2)$^{-1}$
r = rate of desorption CO_2, mol CO_2/(mol amine h)
R_{CO_2} = rate of absorption of CO_2, kmol/(m^2 s)
ΔT = temperature difference between the rich and lean solutions, K
x_{amine} = fraction of amine in the liquid

GREEK SYMBOLS

α = loading capacity, mol CO_2/mol amine
ρ = density of amine solution, kg/m^3
μ = viscosity of amine solution, mPa s

REFERENCES

(1) Vaidya, P. D.; Kenig, E. Y. CO_2-Alkanolamine reaction kinetics: A review of recent studies. *Chem. Eng. Technol.* **2007**, *30*, 1467−1474.
(2) Sartori, G.; Savage, D. Sterically hindered amines for carbon dioxide removal from gases. *Ind. Eng. Chem. Fundam.* **1983**, *22*, 239−249.
(3) Bougie, F.; Iliuta, M. C. Kinetics of absorption of carbon dioxide into aqueous solutions of 2-amino-2-hydroxymethyl-1,3-propanediol. *Chem. Eng. Sci.* **2009**, *64*, 153−162.
(4) Park, J. Y.; Yoon, S. J.; Lee, H. Effect of steric hindrance on carbon dioxide absorption into new amine solutions: Thermodynamic and spectroscopic verification through solubility and NMR analysis. *Environ. Sci. Technol.* **2003**, *37*, 1670−1675.
(5) Park, J. Y.; Yoon, S. J.; Lee, H.; Yoon, J. H.; Shim, J. G.; Lee, J. K.; Min, B. Y.; Eum, H. M. Density, viscosity, and solubility of CO_2 in aqueous solutions of 2-amino-2-hydroxymethyl-1,3-propanediol. *J. Chem. Eng. Data* **2002**, *47*, 970−973.
(6) Ghulam, M.; Mohd, S. A.; Azmi, B. M. Solubility of carbon dioxide in aqueous solution of 2-amino-2-hydroxymethyl-1,3-propanediol at elevated pressures. *Res. J. Chem. Environ.* **2013**, *17*, 41−45.
(7) Oktavian, R.; Taha, M.; Lee, M. J. Experimental and computational study of CO_2 storage and sequestration with aqueous 2-amino-2-hydroxymethyl-1,3-propanediol (TRIS) solutions. *J. Phys. Chem. A* **2014**, *118*, 11572−11582.
(8) Le Tourneux, D.; Iliuta, I.; Iliuta, M. C.; Fradette, S.; Larachi, F. Solubility of carbon dioxide in aqueous solutions of 2-amino-2-hydroxymethyl-1,3-propanediol. *Fluid Phase Equilib.* **2008**, *268*, 121−129.
(9) Murshid, G.; Shariff, A. M.; Lau, K. K.; Bustam, M. A.; Ahmad, F. Physical properties and thermal decomposition of aqueous solutions of 2-amino-2-hydroxymethyl-1,3-propanediol (AHPD). *Int. J. Thermophys.* **2011**, *32*, 2040−2049.
(10) Bougie, F.; Iliuta, M. C. CO_2 absorption into mixed aqueous solutions of 2-amino-2-hydroxymethyl-1,3-propanediol and piperazine. *Ind. Eng. Chem. Res.* **2010**, *49*, 1150−1159.
(11) Dash, S. K.; Samanta, A.; Samanta, A. N.; Bandyopadhyay, S. S. Absorption of carbon dioxide in piperazine activated concentrated aqueous 2-amino-2-methyl propanol solvent. *Chem. Eng. Sci.* **2011**, *66*, 3223−3233.
(12) Sun, W. C.; Yong, C. B.; Li, M. H. Kinetics of the absorption of carbon dioxide into mixed aqueous solutions of 2-amino-2-methyl-l-propanol and piperazine. *Chem. Eng. Sci.* **2005**, *60*, 503−516.
(13) Ume, C. S.; Alper, E.; Gordesli, F. P. Kinetics of carbon dioxide reaction with aqueous mixture of piperazine and 2-amino-2-ethyl-1,3-propanediol. *Int. J. Chem. Kinet.* **2013**, *45*, 161−167.
(14) Gordesli, F. P.; Ume, C. S.; Alper, E. Mechanism and kinetics of carbon dioxide capture using activated 2-amino-2-methyl-1,3-propanediol. *Int. J. Chem. Kinet.* **2013**, *45*, 566−573.
(15) Bougie, F.; Lauzon-Gauthier, J.; Iliuta, M. C. Acceleration of the reaction of carbon dioxide into aqueous 2-amino-2-hydroxymethyl-1,3-propanediol solutions by piperazine addition. *Chem. Eng. Sci.* **2009**, *64*, 2011−2019.
(16) Bougie, F.; Iliuta, I.; Iliuta, M. C. Absorption of CO_2 by AHPD-Pz aqueous blend in PTFE hollow fiber membrane contactors. *Sep. Purif. Technol.* **2014**, *138*, 84−91.
(17) Bougie, F.; Iliuta, I.; Iliuta, M. C. Flat sheet membrane contactor (FSMC) for CO_2 separation using aqueous amine solutions. *Chem. Eng. Sci.* **2015**, *123*, 255−264.
(18) Safdar, R.; Thanabalan, M.; Omar, A. A. Solubility of CO_2 in 20 wt. % aqueous solution of piperazine. *Procedia Eng.* **2016**, *148*, 1377−1379.
(19) Murshid, G.; Garg, S.; Ali, A.; Maqsood, K.; See, T. L. An experimental and modeling approach to investigate CO_2 solubility in blended aqueous solutions of 2-amino-2-hydroxymethyl-1,3-propanediol (AHPD) and piperazine (PZ). *Cleaner Eng. Technol.* **2020**, *1*, No. 100004.
(20) Bougie, F.; Iliuta, M. C. Analysis of regeneration of sterically hindered alkanolamines aqueous solutions with and without activator. *Chem. Eng. Sci.* **2010**, *65*, 4746−4750.
(21) Artanto, Y.; Jansen, J.; Pearson, P.; Puxty, G.; Cottrell, A.; Meuleman, E.; Feron, P. Pilot-scale evaluation of AMP/PZ to capture CO_2 from flue gas of an Australian brown coal-fired power station. *Int. J. Greenhouse Gas Control* **2014**, *20*, 189−195.
(22) Singh, P.; van Swaaij, W. P. M.; Brilman, D. W. F. Energy efficient solvents for CO_2 absorption from flue gas: Vapor liquid equilibrium and pilot plant study. *Energy Procedia* **2013**, *37*, 2021−2046.
(23) Patil, M.; Vaidya, P.; Kenig, E. Bench-scale study for CO_2 capture using AMP/PZ/water mixtures. *Chem. Eng. Trans.* **2018**, *69*, 163−168.
(24) Moioli, S.; Ho, M. T.; Wiley, D. E.; Pellegrini, L. A. Assessment of carbon dioxide capture by precipitating potassium taurate solvent. *Int. J. Greenhouse Gas Control* **2019**, *87*, 159−169.
(25) Liu, H.; Jiang, X.; Idem, R.; Dong, S.; Tontiwachwuthikul, P. Comprehensive reaction kinetics model of CO_2 absorption into 1-dimethylamino-2-propanol. *AIChE J.* **2022**, *68*, No. e17816.
(26) Liu, H.; Jiang, X.; Idem, R.; Dong, S.; Tontiwachwuthikul, P. AI models for correlation of physical properties in system of 1DMA2P-CO_2-H_2O. *AIChE J.* **2022**, *68*, No. e17761.
(27) Quan, H.; Dong, S.; Zhao, D.; Li, H.; Geng, J.; Liu, H. Generic AI models for mass transfer coefficient prediction in amine-based CO_2 absorber, Part II: RBFNN and RF model. *AIChE J.* **2018**, *1*, No. e17904.
(28) Bhatti, U. H.; Nam, S.; Park, S. Y.; Baek, I. H. Performance and mechanism of metal oxide catalyst-aided amine solvent regeneration. *ACS Sustainable Chem. Eng.* **2018**, *6*, 12079−12087.
(29) Caplow, M. Kinetics of carbamate formation and breakdown. *J. Am. Chem. Soc.* **1968**, *90*, 6795−6803.
(30) Danckwerts, P. V. The reaction of CO_2 with ethanolamines. *Chem. Eng. Sci.* **1979**, *34*, 443−446.

https://doi.org/10.1021/acs.energyfuels.2c03909
Energy Fuels 2023, 37, 6651−6660

(31) Patil, M. P.; Vaidya, P. D. New AMP/polyamine blends for improved CO_2 capture: Study of kinetic and equilibrium features. *Can. J. Chem. Eng.* **2020**, *98*, 556−565.
(32) Vaidya, P. D.; Jadhav, S. G. Absorption of carbon dioxide into sterically hindered amines: kinetics analysis and the influence of promoters. *Can. J. Chem. Eng.* **2014**, *92*, 2218−2227.
(33) Sutar, P. N.; Vaidya, P. D.; Kenig, E. Y. Activated DEEA solutions for CO_2 capture-a study of equilibrium and kinetic characteristics. *Chem. Eng. Sci.* **2013**, *100*, 234−241.
(34) Altabash, G.; Al-Hindi, M.; Azizi, F. Intensifying the absorption of CO_2 in water using a static mixer. Part I: Effect of measurement technique. *Ind. Eng. Chem. Res.* **2020**, *59*, 11691−11704.
(35) Artanto, Y.; Jansen, J.; Pearson, P.; Do, T.; Cottrell, A.; Meuleman, E.; Feron, P. Performance of MEA and amine-blends in the CSIRO PCC Pilot Plant at Loy Yang Power in Australia. *Fuel* **2012**, *101*, 264−275.
(36) Jiang, K.; Li, K.; Puxty, G.; Yu, H.; Feron, P. H. M. Information derivation from vapor-liquid equilibria data: A simple shortcut to evaluate the energy performance in an amine-based postcombustion CO_2 capture. *Environ. Sci. Technol.* **2018**, *52*, 10893−10901.
(37) Oexmann, J.; Kather, A. Minimising the regeneration heat duty of post-combustion CO_2 capture by wet chemical absorption: The misguided focus on low heat of absorption solvents. *Int. J. Greenhouse Gas Control* **2010**, *4*, 36−43.
(38) Sarode, U. K.; Vaidya, P. D. On the CO_2 absorption kinetics, loading capacity and catalytic desorption of aqueous solutions of N-methyl-D-glucamine *Can. J. Chem. Eng.* DOI: 10.1002/cjce.24865.
(39) Zhang, X.; Liu, H.; Liang, Z. CO_2 desorption in single and blended amine solvents with and without catalyst. *Energy Procedia* **2017**, *114*, 1862−1868.
(40) Versteeg, G. F.; van Swaaij, W. P. M. Solubility and diffusivity of acid gases (carbon dioxide, nitrous oxide) in aqueous alkanolamine solutions. *J. Chem. Eng. Data* **1988**, *33*, 29−34.
(41) Littel, R. J.; Versteeg, G. F.; van Swaaij, W. P. M. Physical absorption into non-aqueous solutions in a stirred cell reactor. *Chem. Eng. Sci.* **1991**, *46*, 3308−3313.
(42) Konduru, P. B.; Vaidya, P. D.; Kenig, E. Y. Kinetics of removal of carbon dioxide by aqueous solutions of N,N-diethylethanolamine and piperazine. *Environ. Sci. Technol.* **2010**, *44*, 2138−2143.
(43) Ume, C. S.; Ozturk, M. C.; Alper, E. Kinetics of CO_2 absorption by a blended aqueous amine solution. *Chem. Eng. Technol.* **2012**, *35*, 464−468.
(44) Muchan, P.; Narku-Tetteh, J.; Saiwan, C.; Idem, R.; Supap, T.; Tontiwachwuthikul, P. Effect of number of hydroxyl group in sterically hindered alkanolamine on CO_2 capture activity. *Energy Procedia* **2017**, *114*, 1966−1972.
(45) Richner, G.; Puxty, G. Assessing the chemical speciation during CO_2 absorption by aqueous amines using in situ FTIR. *Ind. Eng. Chem. Res.* **2012**, *51*, 14317−14324.
(46) Sun, C.; Dutta, P. K. Infrared spectroscopic study of reaction of carbon dioxide with aqueous monoethanolamine solutions. *Ind. Eng. Chem. Res.* **2016**, *55*, 6276−6283.

https://doi.org/10.1021/acs.energyfuels.2c03909
Energy Fuels 2023, 37, 6651−6660